

Comparison of Convolutional and Turbo Coding For Broadband FWA Systems

Ioannis A. Chatzigeorgiou[†], Miguel R. D. Rodrigues[†], Ian J. Wassell[†] and Rolando A. Carrasco[‡]

[†]Digital Technology Group

Computer Laboratory, University of Cambridge

{ic231,mrdr3,ijw24}@cam.ac.uk

[‡]Communications and Signal Processing Group

School of EE&C Eng., University of Newcastle

r.carrasco@newcastle.ac.uk

Abstract

It has been demonstrated that turbo codes substantially outperform other codes, e.g., convolutional codes, both in the non-fading additive white Gaussian noise (AWGN) channel as well as multiple-transmit and multiple-receive antenna fading channels. Moreover, it has also been reported that turbo codes perform very well in fast fading channels, but perform somewhat poorly on slow and block fading channels of which the broadband fixed wireless access (FWA) channel is an example. In this paper, we thoroughly compare the performance of turbo-coded and convolutional-coded broadband FWA systems both with and without antenna diversity under the condition of identical complexity for a variety of decoding algorithms. In particular, we derive mathematical expressions to characterise the complexity of turbo decoding based on state-of-the-art Log-MAP and Max-Log-MAP algorithms as well as convolutional decoding based on the Viterbi algorithm in terms of the number of equivalent addition operations. Simulation results show that turbo codes do not offer any performance advantage over convolutional codes in FWA systems without antenna diversity or FWA systems with limited antenna diversity. Indeed, turbo codes only outperform convolutional codes in FWA systems having significant antenna diversity.

Keywords – Algorithms, Complexity theory, Communication system performance, Concatenated Coding, Convolutional Codes, Decoding, Fading Channels, Iterative Methods, Trellis Codes.

1 Introduction

Broadband fixed wireless access (FWA) systems enable high data rate communications where traditional landlines are either unavailable or too costly to be installed. These systems also enable operators in a competitive environment to roll-out broadband services in a rapid and cost effective manner [1]. In this context, broadband FWA standardisation activities have been performed under the auspices of the IEEE 802.16 [2] and the ETSI HIPERMAN [3] working groups. In particular, the IEEE 802.16a standard proposes a number of transmission techniques to combat multipath fading in broadband FWA systems, for example orthogonal frequency-division multiplexing (OFDM). This standard also proposes the use of turbo and convolutional channel coding techniques to further improve performance in broadband FWA systems.

Turbo codes have been shown to be very powerful in both the additive white Gaussian noise (AWGN) channel [4,5] as well as in multiple-transmit and multiple-receive antenna Rayleigh fading channels [6-8]. Turbo codes have also been shown to perform very well in rapidly fading channels [9], but to perform less well in slow and block fading channels [10,11], of which the broadband FWA channel is an example. In rapidly fading channels, coding together with interleaving techniques are used to spread consecutive code bits over multiple independently fading blocks to improve performance. However, in slow and block fading channels coding together with interleaving techniques cannot in general be used in an effective manner because delay and latency considerations limit the depth of interleaving. This situation compromises in particular the performance of turbo codes because occasional deep fades cause severe error propagation in the iterative decoding process [12].

Accordingly, comparisons of the performance of turbo and convolutional codes in slow and block fading channels constitutes a topic of practical research interest. In particular, Hoshyar *et al.* have shown that turbo and convolutional codes perform identically in block fading channels with no antenna diversity [10]. In addition, Lin *et al.* have shown that turbo outperform convolutional codes in Rayleigh slow fading channels with antenna diversity only at a high signal-to-noise ratio (SNR) [11].

In this paper, we thoroughly compare the performance of turbo and convolutional codes in broadband FWA systems both with and without antenna diversity. However, this work differs from that in [10] and [11] in that the comparisons are carried out under the condition of identical complexity for a variety of decoding algorithms, including the widely used log-domain maximum *a posteriori* algorithm (Log-MAP) [13] as well as the simplified Max-Log-MAP algorithm [14] for turbo decoding and the conventional Viterbi algorithm [15] for convolutional decoding.

This paper is organised as follows: Section 2 introduces the system model and gives a brief description of the decoding algorithms used for turbo decoding and convolutional decoding, whilst section 3 characterises their complexity. Section 4 compares the performance of turbo and convolutional coding under the condition of identical complexity for a variety of decoding algorithms in broadband FWA systems both with and without antenna diversity. Finally, section 5 summarises the main contributions of this paper.

2 System Model

2.1 General Overview

In this work, we consider systems based on OFDM transmission, which lies at the heart of current broadband FWA standards. We also consider single antenna FWA systems, which do not exploit space diversity, as well as a multiple antenna FWA systems, which do exploit space diversity. Figure 1 depicts the system block diagram, where N_T and N_R represent the number of transmit and receive antennas, respectively.

At the transmitter, the information bits are encoded and block interleaved. We consider both turbo and convolutional encoders. For turbo coding, the encoder consists of the parallel concatenation of two recursive systematic convolutional (RSC) encoders with rate 1/2, as described in [4,5]. Alternate puncturing of the parity bits transforms the conventional 1/3 rate turbo code to a 1/2 rate turbo code. For convolutional coding, the encoder consists of an RSC encoder with rate 1/2. The mapper maps groups of $\log_2 M_s$ bits into one of M_s complex symbols from a unit power M_s -QAM constellation.

In single antenna systems ($N_T = 1$), the space-time processing block does not further process the modulation symbols; instead, the modulation symbols are passed directly to the OFDM block. However, in multiple transmit antenna systems ($N_T > 1$), the space-time processing block will further process the modulation symbols before passing them to the OFDM block. In particular, the space-time processor generates for each particular OFDM sub-carrier a space-time block code (STBC) according to the generator matrices \mathbf{G}_2 , \mathbf{G}_3 or \mathbf{G}_4 given by [16-18]¹

$$\mathbf{G}_2 = \begin{bmatrix} x_1 & x_2 \\ -x_2^* & x_1^* \end{bmatrix}, \quad (1)$$

$$\mathbf{G}_3 = \begin{bmatrix} x_1 & x_2 & x_3 \\ -x_2 & x_1 & -x_4 \\ -x_3 & x_4 & x_1 \\ -x_4 & -x_3 & x_2 \\ x_1^* & x_2^* & x_3^* \\ -x_2^* & x_1^* & -x_4^* \\ -x_3^* & x_4^* & x_1^* \\ -x_4^* & -x_3^* & x_2^* \end{bmatrix}, \quad (2)$$

$$\mathbf{G}_4 = \begin{bmatrix} x_1 & x_2 & x_3 & x_4 \\ -x_2 & x_1 & -x_4 & x_3 \\ -x_3 & x_4 & x_1 & -x_2 \\ -x_4 & -x_3 & x_2 & x_1 \\ x_1^* & x_2^* & x_3^* & x_4^* \\ -x_2^* & x_1^* & -x_4^* & x_3^* \\ -x_3^* & x_4^* & x_1^* & -x_2^* \\ -x_4^* & -x_3^* & x_2^* & x_1^* \end{bmatrix}, \quad (3)$$

¹ Here, we consider space-time coded OFDM systems where redundancy spans space and time domains [19], rather than space-frequency coded OFDM systems where redundancy spans space and frequency domains [20,21].

where x_1, x_2, x_3 and x_4 denote modulation symbols. The rows of the matrices represent symbols transmitted in different time slots by a particular OFDM sub-carrier. The columns of the matrices represent symbols transmitted by different antennas again by the particular OFDM sub-carrier. Essentially, a total of $K \times N_T$ symbols obtained from the original K' modulation symbols are transmitted during K separate time slots by N_T transmit antennas by each particular OFDM sub-carrier. Note that $\mathbf{G}_2, \mathbf{G}_3$ and \mathbf{G}_4 are appropriate for two, three and four transmit antennas, respectively, and for an arbitrary number of receive antennas. Note also that \mathbf{G}_2 is rate $K'/K = 1$, whereas \mathbf{G}_3 and \mathbf{G}_4 are rate $K'/K = 1/2$. Single antenna systems (where $N_T = 1$ and $K' = K = 1$) are a special case of multiple transmit antenna systems (where $N_T > 1$ and $K', K > 1$). Thus, in the sequel both single as well as multiple antenna systems are treated under the same framework.

Finally, at each transmit antenna chain, N complex symbols corresponding to the elements for a particular time slot for the N different STBC are imposed onto N orthogonal sub-carriers by means of an IFFT, a cyclic prefix is inserted with duration longer than the impulse response of the channel to combat intersymbol interference (ISI) and intercarrier interference (ICI), and finally the signal is digital-to-analogue converted.

The OFDM signal is distorted by a broadband FWA channel as well as AWGN. The broadband FWA channel is time-dispersive but not significantly time-varying. Hence, we assume that the channel is essentially constant during the transmission of a frame of data.

At the receiver, at each receive antenna chain the signal is analogue-to-digital converted, the cyclic prefix is removed, and the N complex symbols corresponding to the elements for a particular time slot for the N different STBC are removed from the N orthogonal sub-carriers by means of an FFT.

The relation between the complex receive symbols and the complex transmit symbols associated with the STBC conveyed by the n th OFDM sub-carriers can be written as follows²

$$\mathbf{R}_n = \mathbf{H}_n \mathbf{S}_n + \mathbf{N}_n, \quad (4)$$

where

$$\mathbf{R}_n = \begin{bmatrix} R_n^1(1) & R_n^1(2) & \cdots & R_n^1(K) \\ R_n^2(1) & R_n^2(2) & \cdots & R_n^2(K) \\ \vdots & \vdots & \ddots & \vdots \\ R_n^{N_R}(1) & R_n^{N_R}(2) & \cdots & R_n^{N_R}(K) \end{bmatrix}, \quad (5)$$

$$\mathbf{S}_n = \begin{bmatrix} S_n^1(1) & S_n^1(2) & \cdots & S_n^1(K) \\ S_n^2(1) & S_n^2(2) & \cdots & S_n^2(K) \\ \vdots & \vdots & \ddots & \vdots \\ S_n^{N_T}(1) & S_n^{N_T}(2) & \cdots & S_n^{N_T}(K) \end{bmatrix}, \quad (6)$$

$$\mathbf{N}_n = \begin{bmatrix} N_n^1(1) & N_n^1(2) & \cdots & N_n^1(K) \\ N_n^2(1) & N_n^2(2) & \cdots & N_n^2(K) \\ \vdots & \vdots & \ddots & \vdots \\ N_n^{N_R}(1) & N_n^{N_R}(2) & \cdots & N_n^{N_R}(K) \end{bmatrix}, \quad (7)$$

and

$$\mathbf{H}_n = \begin{bmatrix} H_n^{1,1} & H_n^{1,2} & \cdots & H_n^{1,N_t} \\ H_n^{2,1} & H_n^{2,2} & \cdots & H_n^{2,N_t} \\ \vdots & \vdots & \ddots & \vdots \\ H_n^{N_r,1} & H_n^{N_r,2} & \cdots & H_n^{N_r,N_t} \end{bmatrix}. \quad (8)$$

² Here, we focus without loss of generality on the first space-time block code frame.

Now, $R_n^j(k)$ denotes the complex receive symbol associated with the n th OFDM sub-carrier at time slot k and receive antenna j , $S_n^i(k)$ denotes the complex transmit symbol associated with the n th OFDM sub-carrier at time slot k and transmit antenna i , $H_n^{i,j}$ is the unit power random channel frequency response at the n th OFDM sub-channel from transmit antenna i to receive antenna j (note that $H_n^{i,j}$ is independent of time slot k), and $N_n^j(k)$ denotes the noise random variable at the n th OFDM sub-channel at time slot k and receive antenna j . The noise random variables are uncorrelated circularly symmetric complex Gaussian with mean zero and variance $1/\text{SNR}_{\text{norm}}$, where $\text{SNR}_{\text{norm}} = \text{SNR}/N_T$ and SNR denotes the average signal-to-noise ratio per receive antenna.

Next, the complex symbols are demapped into soft bits. In particular, the soft demapper computes the log-likelihood ratio (LLR) given by

$$L_D(b_n^m(k)|\mathbf{R}_n) = \ln \frac{\text{Prob}\{b_n^m(k) = 1 | \mathbf{R}_n\}}{\text{Prob}\{b_n^m(k) = 0 | \mathbf{R}_n\}}, \quad (9)$$

where $b_n^m(k)$ is the m th bit conveyed by the k th modulation symbol associated with the STBC conveyed by the n th OFDM sub-carrier. The LLR in (9) is also given by

$$\begin{aligned} L_D(b_n^m(k)|\mathbf{R}_n) &= \ln \frac{\sum_{\mathbf{S}_n \in \mathcal{S}^+} p(\mathbf{R}_n | \mathbf{S}_n) \text{Prob}\{\mathbf{S}_n\}}{\sum_{\mathbf{S}_n \in \mathcal{S}^-} p(\mathbf{R}_n | \mathbf{S}_n) \text{Prob}\{\mathbf{S}_n\}} = \ln \frac{\sum_{\mathbf{S}_n \in \mathcal{S}^+} p(\mathbf{R}_n | \mathbf{S}_n) \prod_{m'=1}^{\log_2 M} \prod_{k'=1}^{K'} \text{Prob}\{b_n^{m'}(k')\}}{\sum_{\mathbf{S}_n \in \mathcal{S}^-} p(\mathbf{R}_n | \mathbf{S}_n) \prod_{m'=1}^{\log_2 M} \prod_{k'=1}^{K'} \text{Prob}\{b_n^{m'}(k')\}} \\ &= \ln \frac{\text{Prob}\{b_n^m(k) = 1\}}{\text{Prob}\{b_n^m(k) = 0\}} + \ln \frac{\sum_{\mathbf{S}_n \in \mathcal{S}^+} p(\mathbf{R}_n | \mathbf{S}_n) \prod_{\substack{m', k' \neq m, k \\ m'=1 \\ k'=1}}^{\log_2 M} \prod_{k'=1}^{K'} \text{Prob}\{b_n^{m'}(k')\}}{\sum_{\mathbf{S}_n \in \mathcal{S}^-} p(\mathbf{R}_n | \mathbf{S}_n) \prod_{\substack{m', k' \neq m, k \\ m'=1 \\ k'=1}}^{\log_2 M} \prod_{k'=1}^{K'} \text{Prob}\{b_n^{m'}(k')\}}, \quad (10) \\ &\quad \underbrace{\hspace{10em}}_{\text{extrinsic information, } L_E(b_n^m(k)|\mathbf{R}_n)} \end{aligned}$$

where S^+ is the set of matrices of transmit symbols \mathbf{S}_n such that $b_n^m(k)=1$ (i.e., $S^+ = \{\mathbf{S}_n : b_n^m(k)=1\}$), S^- is the set of matrices of transmit symbols \mathbf{S}_n such that $b_n^m(k)=0$ (i.e., $S^- = \{\mathbf{S}_n : b_n^m(k)=0\}$), and the probability density function $p(\mathbf{R}_n|\mathbf{S}_n)$ is given by

$$p(\mathbf{R}_n|\mathbf{S}_n) = \frac{1}{(2\pi \cdot N_T \cdot \text{SNR}^{-1})^{KN_R}} e^{-\frac{(\mathbf{R}_n - \mathbf{H}_n \mathbf{S}_n)^H (\mathbf{R}_n - \mathbf{H}_n \mathbf{S}_n)}{N_T \cdot \text{SNR}^{-1}}}. \quad (11)$$

Note that the log-likelihood ratio is the sum of the *a priori* information and the extrinsic information, i.e.,

$$L_D(b_n^m(k)|\mathbf{R}_n) = L_A(b_n^m(k)) + L_E(b_n^m(k)|\mathbf{R}_n). \quad (12)$$

The *a priori* information is equal to zero, i.e.,

$$L_A(b_n^m(k)) = 0. \quad (13)$$

The extrinsic information can be further simplified for particular modulation schemes as well as STBC by virtue of the orthogonal properties of \mathbf{G}_2 , \mathbf{G}_3 and \mathbf{G}_4 . For example, in the single antenna case ($N_T = N_R = 1$) with no STBC ($K' = K = 1$) and with Gray coded QPSK modulation ($\log_2 M = 2$) it follows that

$$L_E(b_n^1(1)|R_n^1(1)) = 4 \cdot \text{SNR} \cdot |H_n^{1,1}| \cdot \text{Re}\left\{e^{-j\angle H_n^{1,1}} R_n^1(1)\right\}, \quad (14)$$

$$L_E(b_n^2(1)|R_n^1(1)) = 4 \cdot \text{SNR} \cdot |H_n^{1,1}| \cdot \text{Im}\left\{e^{-j\angle H_n^{1,1}} R_n^1(1)\right\}. \quad (15)$$

In the multiple antenna case ($N_T = 2, N_R > 1$) with the STBC specified by \mathbf{G}_2 ($K' = K = 2$) and with Gray coded QPSK modulation ($\log_2 M = 2$) it follows that

$$L_E(b_n^1(1)|\mathbf{R}_n) = 4 \cdot \text{SNR} \cdot \text{Re}\left\{\sum_{n_r=1}^{N_R} (H_n^{1,n_r})^* \cdot R_n^{n_r}(1) + H_n^{2,n_r} \cdot (R_n^{n_r}(2))^*\right\}, \quad (16)$$

$$L_E(b_n^2(1)|\mathbf{R}_n) = 4 \cdot \text{SNR} \cdot \text{Im}\left\{\sum_{n_r=1}^{N_R} (H_n^{1,n_r})^* \cdot R_n^{n_r}(1) + H_n^{2,n_r} \cdot (R_n^{n_r}(2))^*\right\}, \quad (17)$$

$$L_E(b_n^1(2)|\mathbf{R}_n) = 4 \cdot \text{SNR} \cdot \text{Re} \left\{ \sum_{n_r=1}^{N_R} (H_n^{2,n_r})^* \cdot R_n^{n_r}(1) - H_n^{1,n_r} \cdot (R_n^{n_r}(2))^* \right\}, \quad (18)$$

$$L_E(b_n^2(2)|\mathbf{R}_n) = 4 \cdot \text{SNR} \cdot \text{Im} \left\{ \sum_{n_r=1}^{N_R} (H_n^{2,n_r})^* \cdot R_n^{n_r}(1) - H_n^{1,n_r} \cdot (R_n^{n_r}(2))^* \right\}. \quad (19)$$

Note that similar extrinsic information expressions can also be determined for other particular modulation schemes and STBCs.

Finally, the soft bits (the LLRs) are block de-interleaved and decoded. For turbo coding, the constituent soft-input soft-output decoders use either the optimal log-MAP algorithm [13] or the max-log-MAP algorithm [14]. For convolutional coding, the decoder uses the conventional Viterbi algorithm [15].

2.2 Decoders Overview

We now describe the basic ideas behind the various decoding algorithms that are necessary for the complexity computations. We initially consider the Viterbi algorithm used for systems based on convolutional codes. Subsequently, we consider both the log-MAP and the max-log-MAP algorithms used for systems based on turbo codes.

2.2.1 Viterbi Algorithm

The *Viterbi algorithm* [15] estimates the most probable sequence of states for a received sequence of soft bits. A branch in the trellis diagram of the convolutional code corresponds to a transition from a memory state s' at time $t-1$ to another state s at time step t . The *branch metric* $BM_t^{(s',s)}$ corresponds to the sum of the inner products between the codeword bits associated with the branch and the received soft bits at time step t . Moreover, a path in the trellis diagram corresponds to a series of interconnected branches. The *path metric* corresponds to the sum of the branch metrics of the branches that compose the path. As the path progresses through the trellis,

subsequent branches join the path so that the path metric changes accordingly. If two paths merge to a state s at a time step t , the Viterbi algorithm selects the path with the highest metric, the *survivor path*, and disregards those with lower metrics. The path metric of the survivor path at a time step t for a state s , $PM_t^{(s)}$, is given by

$$PM_t^{(s)} = \max(PM_{t-1}^{(s')} + BM_t^{(s',s)}, PM_{t-1}^{(s'')} + BM_t^{(s'',s)}), \quad (20)$$

where s' and s'' correspond to the states of the competing paths at time step $t-1$. This add-compare-and-select process yields maximum likelihood (ML) decisions.

2.2.2 BCJR algorithm

Although the Viterbi algorithm yields ML decisions, it can neither produce reliability values (LLRs) associated with the output decoded bits nor it can exploit a priori information associated with the input information bits. However, these two processes are of utmost importance to enable the constructive information exchange between the two component decoders for successful iterative decoding of turbo codes. Berrou *et al.* [4] have proposed the use of a maximum a posteriori (MAP) decoding algorithm based on the widely known *BCJR algorithm* [22] for each component decoder in a turbo decoder. In particular, the BCJR algorithm yields the following reliability values for a decoded bit at time step t

$$L_D(b_t) = \ln \sum_{\substack{(s',s): \\ b_t=+1}} \alpha_{t-1}(s') \gamma_t(s',s) \beta_t(s) - \ln \sum_{\substack{(s',s): \\ b_t=-1}} \alpha_{t-1}(s') \gamma_t(s',s) \beta_t(s), \quad (21)$$

where the terms $\alpha_{t-1}(s')$ and $\beta_t(s)$ are derived by means of a forward and a backward recursion, respectively, based on

$$\begin{aligned} a_t(s) &= \sum_{\forall s'} a_{t-1}(s') \gamma_t(s',s), \\ \beta_{t-1}(s') &= \sum_{\forall s} \beta_t(s) \gamma_t(s',s), \end{aligned} \quad (22)$$

and the term $\gamma_t(s', s)$ is calculated by considering both the branch metric at time step t and the a priori information for the decoded bit, as described in more detail in [22]. The BCJR algorithm is considered to be extremely complex owing to the various multiplication operations as well as the logarithmic operations required to compute the a-posteriori LLR for each decoded bit. However, two simple modifications were proposed to reduce its complexity without severely compromising performance.

2.2.3 Log-MAP and Max-log-MAP algorithms

The first modification to the BCJR algorithm yields the max-log-MAP algorithm proposed by Koch and Baier in 1990 [14]. This modification is based on the calculation of the a-posteriori LLR by using the approximation

$$\ln(e^{\lambda_1} + e^{\lambda_2}) \approx \max(\lambda_1, \lambda_2). \quad (23)$$

Consequently, expressions (21) and (22) are considerably simplified, since the overall number of operations decreases and moreover multiplications are transformed into additions in the log-domain. However, this modification results in consideration of only the ML path in the trellis through a particular state, rather than every path in trellis through this state [13]. Therefore, the performance of the max-log-MAP algorithm is inferior to that of the BCJR algorithm.

Another modification yields the log-MAP algorithm proposed by Robertson *et al.* in 1995 [13]. This modification is based on the correction of the approximation by using the Jacobian logarithm, that is

$$\ln(e^{\lambda_1} + e^{\lambda_2}) = \max(\lambda_1, \lambda_2) + \ln(1 + e^{-|\lambda_1 - \lambda_2|}). \quad (24)$$

Note that since the correction term takes only a limited number of values, look-up tables can be used to reduce the complexity of the computations. Otherwise, if the correction term is computed exactly, this (exact) log-MAP algorithm is entirely equivalent to the BCJR algorithm.

3 Complexity Considerations

We now consider the characterization of the complexity of the various decoding algorithms. We will follow the conventional approach in the field of coding theory, where the complexity of a decoding algorithm is measured in terms of the total number of computational operations [13,23], such as additions, subtractions, multiplications and divisions. In particular, similarly to [24], we express the complexity of the various basic operations in terms of that of an addition operation. Hence, we ultimately express the complexity of log-MAP, max-log-MAP and the Viterbi decoding algorithms in terms of the total number of equivalent additions executed. This approach delivers results with wider applicability, since the complexity measure is not tied to specific hardware implementations.

The basic operations performed by the various decoding algorithms include addition (ADD), subtraction (SUB), multiplication by ± 1 (MUL), division by 2 (DIV), comparison (CP), $\max(x,y)$ or $\min(x,y)$ (MAX) and table look-up (LKUP). The ADD, SUB, MUL, DIV and CP operations correspond to one equivalent addition, whilst the MAX operation corresponds to two equivalent additions, since it first uses a CP operation to compare the two input values and then stores the result in a register [24]. The LKUP operation corresponds to three equivalent additions because no more than three CP operations are required to map an input value to one of the eight values stored in the look-up table [13] for the close approximation of the exponential factor in (24). The procedures performed by the log-MAP and the max-log-MAP algorithms can be classified as follows [13,22]:

- Branch Metrics Calculation (Proc. A)
- Forward Metrics Calculation (Proc. B)
- Backward Metrics Calculation (Proc. C)
- Soft Decision of the decoded bit (Proc. D)

In the case of max-log-MAP, procedures B, C and D require implementation of the MAX function. In the case of log-MAP, these procedures also require the implementation of the MAX function plus one ADD, one SUB and one LKUP operations.

The procedures performed by the Viterbi algorithm can be classified as follows [15]:

- Branch Metrics Calculation (Proc. A)
- Path Metrics Update (Proc. E)
- Hard Decision Generation (Proc. G)

Moreover, in this case procedure A does not exploit any *a priori* information.

Tables 1-3 summarize the computational requirements of the various decoding algorithms as a function of the encoder memory order M . Note that here we assume that the constituent RSC encoders for turbo coding, as well as the RSC encoder for convolutional coding are rate 1/2. Note that we also take into account the additional complexity associated with the branch metrics calculations due to *a priori* information exploited by the turbo decoder. Finally, Table 4 summarizes the overall complexity (in terms of the number of equivalent addition operations) of the various decoding algorithms.

As an example, let us consider in detail the computational requirements of the Viterbi algorithm for a rate 1/2 convolutional code (see Table 3). Calculation of a branch metric requires 2 MUL operations for the computation of the two inner products between the codeword bits associated with the branch and the received soft bits, and 1 ADD operation for the summation of the two products. Hence, procedure A requires 4×2^M MUL and 2×2^M ADD operations, given that two branches emerge from each of the 2^M states per time step. Moreover, calculation of a path metric requires 2 ADD and 1 MAX operations (see (20)). Consequently, procedure E requires 2×2^M ADD and 2^M MAX operations per time step. Finally, procedure G requires only 1 LKUP operation for the generation of a hard bit per time step, as explained in [24].

Figure 2 compares the complexity of turbo decoding and convolutional decoding for particular configurations. As an example, we note that the complexity of a turbo decoder with memory order $M = 2$ applying the log-MAP algorithm with 7 iterations, is comparable to that of a similar turbo decoder applying the max-log-MAP algorithm with 11 iterations, or to that of a convolutional decoder with memory order $M = 8$ applying the conventional Viterbi algorithm.

Finally, we note that Wu [24] has also previously analysed the complexity of various decoding algorithms in terms of the number of equivalent addition operations. However, our analysis differs from that presented in [24] in one fundamental aspect. We take the complexity of a look-up operation to be equivalent to 3 equivalent addition operations, rather than the 6 equivalent addition operations considered in [24]. Hence, our results are less pessimistic in terms of the number of equivalent addition operations than those in [24]. We also note that Robertson *et al.* [13] have also previously analysed the complexity of a variety of decoding algorithms, but for simplicity mathematical and logical operations were assumed to exhibit identical complexity.

4 Simulation Results

In our simulations, the convolutional encoder uses an RSC encoder with rate $1/2$, generator polynomial $(1, 753/561)$ and memory order $M = 8$. The number of information bits fed to the convolutional encoder is 1016, so that the number of encoded bits is 2048. The turbo encoder uses two identical terminated RSC encoders with rate $1/2$, octal generator polynomial $(1, 5/7)$ and memory order $M = 2$, and a random interleaver with size either $L = 1021$ or $L = 4093$. Alternate puncturing of the parity bits transforms the conventional $1/3$ rate turbo code to a $1/2$ rate turbo code. In this case, the number of information bits fed to the turbo encoder is either 1021 (for $L = 1021$) or 4093 (for $L = 4093$), so that the number of encoded bits is 2048 or 8192, respectively. The convolutional decoder uses the Viterbi algorithm. The turbo decoder uses either the log-MAP algorithm with 7 iterations or the max-log-MAP algorithm with 11 iterations. Note that these configurations have identical decoding complexity. The depth of the

block interleaver and de-interleaver is set to be equal to 64. In our simulations, we also use OFDM/QPSK signals with OFDM symbol duration $T = 12.8 \mu\text{s}$, cyclic prefix duration $T_{CP} = 3.2 \mu\text{s}$, and $N = 256$ sub-carriers. Furthermore, in the simulations we focus on single antenna as well as multiple antenna systems based on STBCs specified by \mathbf{G}_2 , \mathbf{G}_3 and \mathbf{G}_4 . Six interim broadband FWA channel models have been adopted by the IEEE 802.16a standard [25]. We consider the SUI3 model, which corresponds to average suburban conditions. This model includes three fading taps with delays 0 μs , 0.5 μs and 1.0 μs , with relative powers 0 dB, -5 dB and -10 dB, and with K-factors 1, 0 and 0, respectively. The delay spread is 0.264 μs and the Doppler spread per tap is 0.4 Hz³. The SUI3 channel model specifies an antenna correlation coefficient value equal to 0.4. However, in the simulations we will assess systems both with and without antenna correlation.

Figure 3 compares the performance of various turbo-coded and convolutional-coded systems for both single and multiple antenna configurations for the case of frames having 2048 encoded bits. Here, we set the antenna envelope correlation coefficient to be equal to the nominal value of 0.4. We note that turbo codes substantially outperform convolutional codes in the AWGN channel. However, the performance of turbo codes is similar to that of convolutional codes in single antenna broadband FWA systems. Moreover, the performance of turbo codes is also similar to that of convolutional codes in multiple antenna broadband FWA systems. In particular, we note that this is essentially the case for turbo coding based on both the log-MAP as well as the max-log-MAP algorithms. These results are due to the limited diversity offered both by single antenna as well as multiple antenna FWA channels. In single antenna FWA channels there is no time diversity due to the very slow time variation nature of the channel, and there is only mild frequency diversity due to the mild time-dispersive nature of the channel. In multiple antenna

³ We assume that the channel is essentially constant during the transmission of a frame of data by virtue of the low Doppler spread value. The error rate results are averaged over 10000 channel realisations.

systems, antenna correlation will also substantially limit the advantage owing to space diversity. Hence, the presence of frequent deep fades significantly impairs the performance of turbo codes owing to severe error propagation in the iterative decoding process [12].

Figure 4 also compares the performance of various turbo-coded and convolutional-coded systems for both single and multiple antenna configurations again for the case of frames having 2048 encoded bits. However, here we set the antenna envelope correlation coefficient to be equal to zero, i.e., the ideal situation. In this case, as the number of antennas is increased (i.e. as antenna diversity is increased), turbo codes eventually substantially outperform convolutional codes. In fact, as the number of antennas is increased the underlying fading channel will approach a non-fading AWGN channel, where turbo codes are known to substantially outperform convolutional codes.

Figure 5 and Figure 6 compare the performance of turbo-coded systems for various single antenna and multiple antenna system configurations for frame lengths of 2048 and 8192 encoded bits. Figure 5 applies to systems with an antenna envelope correlation coefficient of 0.4, whereas Figure 6 applies to systems with zero antenna envelope correlation coefficient. In AWGN channels an increase in the length of the turbo code frame, i.e., an increase in the length of the random interleaver employed by the turbo encoder, gives rise to substantial performance improvements. In contrast, an increase in the length of the convolutional code frame does not generally result in performance improvements [15]. Yet, we note that in broadband FWA channels the length of the frame does not change the nature of the previous trends. In particular, in low diversity FWA systems (i.e., systems with a low number of antennas) turbo codes with different frame lengths perform identically. In high diversity FWA systems (i.e., systems with a high number of antennas) turbo codes with a longer frame outperform turbo codes with a shorter frame, and consequently also outperform convolutional codes.

To conclude, we observe that very high order diversity systems are required for turbo-coded systems to outperform convolutional-coded systems. However, this may be difficult to achieve in

FWA systems for various practical and economic reasons. Specifically, the FWA channel is not significantly time-dispersive or time-varying and consequently cannot offer much frequency or time diversity. Moreover, antenna correlation severely limits spatial diversity. Additional results (not presented here) also suggest that the trends observed for the specific turbo and convolutional codes considered in this work also apply to other turbo and convolutional codes with identical complexity.

5 Conclusions

In this paper, we have compared the performance of turbo-coded and convolutional-coded broadband FWA systems both with and without antenna diversity under the condition of identical complexity for a variety of decoding algorithms. We have shown that turbo coding does not offer any performance advantage over convolutional coding for FWA systems without antenna diversity or for FWA systems with limited antenna diversity. We have also shown that turbo coding only outperforms convolutional coding in FWA systems having significant antenna diversity. These results are of practical interest for the deployment and design of high performance broadband FWA systems.

References

- [1] H. Bölcskei, A. J. Paulraj, K. V. S. Hari, R. U. Nabar and W. W. Lu, "Fixed broadband wireless access: State of the art, challenges and future directions," *IEEE Communications Magazine*, vol. 39, pp.100-108, January 2001.
- [2] IEEE Standard, "Part 16: Air interface for fixed broadband wireless access systems – Amendment 2: Media access control modifications and additional physical layer specifications for 2-11 GHz," IEEE 802.16a, January 2003.
- [3] ETSI Standard, "Broadband radio access networks (BRAN); HiperMAN; Physical (PHY) layer," ETSI TS 102 177 V1.2.1, January 2005.
- [4] C. Berrou, A. Glavieux and P. Thitimajshima, "Near Shannon limit error-correcting coding and decoding: Turbo-codes," *Proceedings of the IEEE International Conference on Communications*, vol. 2, pp. 1064-1070, May 1993.
- [5] C. Berrou and A. Glavieux, "Near optimum error correcting coding and decoding: Turbo codes," *IEEE Transactions on Communications*, vol. 44, pp. 1261-1271, October 1996.
- [6] A. Stefanov and T. M. Duman, "Turbo coded modulation for wireless communications with antenna diversity," *Proceedings of the IEEE Vehicular Technology Conference-Fall*, vol. 3, pp. 1565-1569, September 1999.
- [7] A. Stefanov and T. M. Duman, "Turbo coded modulation for systems with transmit and receive antenna diversity," *Proceedings of the IEEE Global Telecommunications Conference*, vol. 5, pp. 2336-2340, November 1999.
- [8] A. Stefanov and T. M. Duman, "Turbo-coded modulation for systems with transmit and receive antenna diversity over block fading channels: system model, decoding approaches, and practical considerations," *IEEE Journal on Selected Areas in Communications*, vol. 19, pp. 958-968, May 2001.
- [9] J. P. Woodard and L. Hanzo, "Comparative study of turbo decoding techniques: An overview," *IEEE Transactions on Vehicular Technology*, vol. 49, pp. 2208-2233, November 2000.

- [10] R. Hoshyar, S. H. Jamali and A. R. S. Bahai, "Turbo coding performance in OFDM packet transmission," *Proceedings of the IEEE Vehicular Technology Conference-Spring*, Tokyo, Japan, vol. 2, pp. 805-810, May 2000.
- [11] L. Lin, L. J. Cimini and C. I. Chuang, "Comparison of convolutional and turbo codes for OFDM with antenna diversity in high-bit-rate wireless applications," *IEEE Communications Letters*, vol.4, pp. 277-279, September 2000.
- [12] H. El Gamal and A. R. Hammons, Jr., "Analyzing the turbo decoder using the Gaussian approximation," *IEEE Transactions on Information Theory*, vol. 47, pp. 671-686, February 2001.
- [13] P. Robertson, E. Villebrun and P. Höeher, "A comparison of optimal and sub-optimal MAP decoding algorithms operating in the log domain," *Proceedings of the IEEE International Conference on Communications*, vol. 2, pp. 1009-1013, June 1995.
- [14] W. Koch and A. Baier, "Optimum and sub-optimum detection of coded data distributed by time-varying inter-symbol interference," in *Proc. IEEE Conference on Global Communications*, San Diego, CA, pp. 1679-1684, December 1990.
- [15] J. G. Proakis. *Digital Communications*, 4th ed. New York: McGraw-Hill, 2001.
- [16] S. M. Alamouti, "A simple transmitter diversity scheme for wireless communications," *IEEE Journal on Selected Areas in Communications*, vol. 16, pp. 1451-1458, October 1998.
- [17] V. Tarokh, H. Jafarkhani and A. R. Calderbank, "Space-time block codes from orthogonal designs," *IEEE Transactions on Information Theory*, vol. 45, pp. 1456-1467, July 1999.
- [18] V. Tarokh, H. Jafarkhani and A. R. Calderbank, "Space-time block coding for wireless communications: Performance results," *IEEE Journal on Selected Areas in Communications*, vol. 17, pp. 451-460, March 1999.
- [19] D. Agrawal, V. Tarokh, A. Naguib and N. Seshadri, "Space-time coded OFDM for high data-rate wireless communication over wideband channels," *Proceedings of the IEEE Vehicular Technology Conference*, vol. 3, pp. 2232-2236, May 1998.
- [20] H. Bölcskei and A. J. Paulraj, "Space-frequency coded broadband OFDM systems," *Proceeding of the IEEE Wireless Communications and Networking Conference*, vol. 1, pp. 1-6, September 2000.

- [21] B. Lu and X. Wang, "Space-time code design in OFDM systems," *Proceedings of the Global Telecommunications Conference*, vol. 2, pp. 1000-1004, November-December 2000.
- [22] L. R. Bahl, J. Cocke, F. Jelinek and J. Raviv, "Optimal decoding of linear codes for minimizing symbol error rate," *IEEE Transactions on Information Theory*, vol. 20, pp. 284-287, March 1974.
- [23] M. P. C. Fossorier, "Iterative Reliability-Based Decoding for Low Density Parity Check Codes", *IEEE Journal on Selected Areas in Communications*, vol. 19, pp. 908-917, May 2001.
- [24] P. H.-Y. Wu, "On the complexity of turbo decoding algorithms," *Proceedings of the IEEE Vehicular Technology Conference-Spring*, vol. 2, pp. 1439-1443, May 2001.
- [25] V. Erceg *et al.*, "Channel Models for Fixed Wireless Applications", IEEE 802.16a cont. IEEE 802.16.3c-01/29r4, June 2003.

Biographies



IOANNIS A. CHATZIGEORGIOU (ic231@cam.ac.uk) is currently a Ph.D. candidate in communication engineering at the University of Cambridge. From 2000 to 2002, he held positions in Marconi Communications and Inmarsat Ltd. He received his Dipl.-Ing in electrical engineering from Democritus University of Thrace, Greece, in 1997 and his M.Sc. in satellite communication engineering from the University of Surrey, U.K., in 2000. His research interests include channel coding, space-time coding and equalization techniques for fixed wireless access systems. He is a Member of the IEEE and the Technical Chamber of Greece.



MIGUEL R. D. RODRIGUES (mrdr3@cam.ac.uk) was born in Porto, Portugal on May 30, 1975. He received the *Licenciatura* degree in electrical engineering from the Faculty of Engineering of the University of Porto, Portugal in 1998 and the Ph.D. degree in electronic and electrical engineering from University College London, U.K. in 2002. He has held postdoctoral research appointments at Cambridge University, U.K., and at Princeton University, U.S.A., in the period from 2003 to 2006. He joined the faculty of the Department of Computer Science, Faculty of Sciences of the University of Porto in 2007. His research interests include information theory, communications theory and signal processing and their applications to wireless systems. He has over 50 publications in international journals and conference proceedings in these areas. He is also a Visiting Researcher at University College London, U.K. Dr. Rodrigues has been the recipient of doctoral and postdoctoral fellowships from the Portuguese Foundation for Science and Technology, a postdoctoral fellowship from Fundação

Calouste Gulbenkian, the Prize Engenheiro António de Almeida, the Prize Engenheiro Cristiano Spratley, and the Merit Scholarship from the University of Porto.



IAN J. WASSELL (ijw24@cam.ac.uk) was born in Wolverhampton, England on October 22, 1960. He received the B.Sc., B.Eng. (Honours) degree (First Class) in electrical and electronic engineering from the University of Loughborough, UK in 1983 and the Ph.D. degree in electronic and electrical engineering from the University of Southampton, U.K. in 1990. He is a Senior University Lecturer at the Computer Laboratory, University of Cambridge. Prior to this he has held positions at the University of Huddersfield, Hutchison Personal Communications Ltd., Multiple Access Communications Ltd. and Marconi Ltd. His research interests include fixed wireless access systems, radio propagation and signal processing. Dr. Wassell is a Member of the Institution of Engineering and Technology.



ROLANDO A. CARRASCO (r.carrasco@newcastle.ac.uk) received the B.Sc. (Honours) degree from the University of Santiago, Chile, and the Ph.D. degree for his work on implementing digital filters using several processors, from the University of Newcastle-upon-Tyne, U.K. He was awarded the IEE Heaviside Premium in 1982 for his work in multiprocessor systems. Between 1982 and 1984 he was employed by Alfred Peters Limited, Sheffield (now Meditech) and carried out research and development in signal processing associated with cochlear stimulation and response. He has been with Staffordshire University since 1984 and is now Professor of Mobile Communications at the University of Newcastle-upon-Tyne. His principle research interests are digital signal processing algorithms for mobile and network communication systems and speech processing/recognition. Professor Carrasco has over a hundred scientific publications, five chapters in telecommunication

reference texts and a patent to his name. He is a member of several organizing committees, a member of the EPSRC College and a member of the EPSRC assessment panel. He is a Fellow of the Institution of Engineering and Technology.

Figures

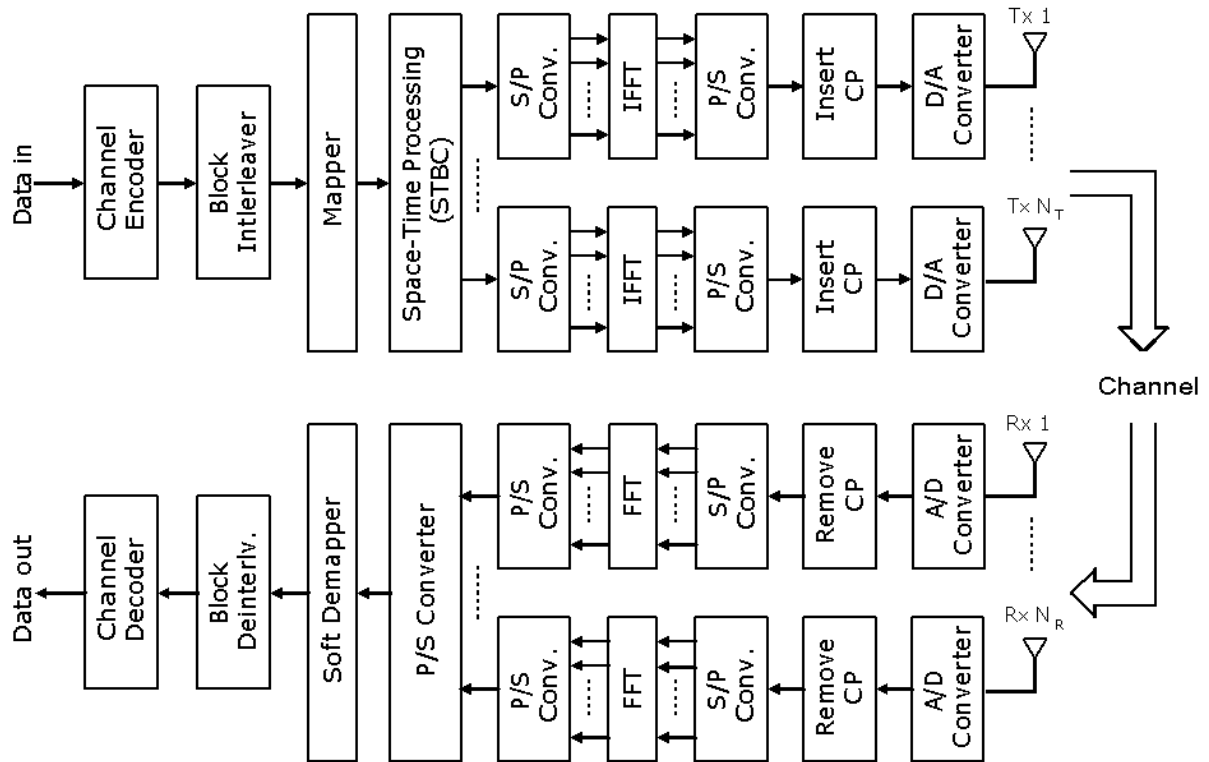


Figure 1: Communications system model.

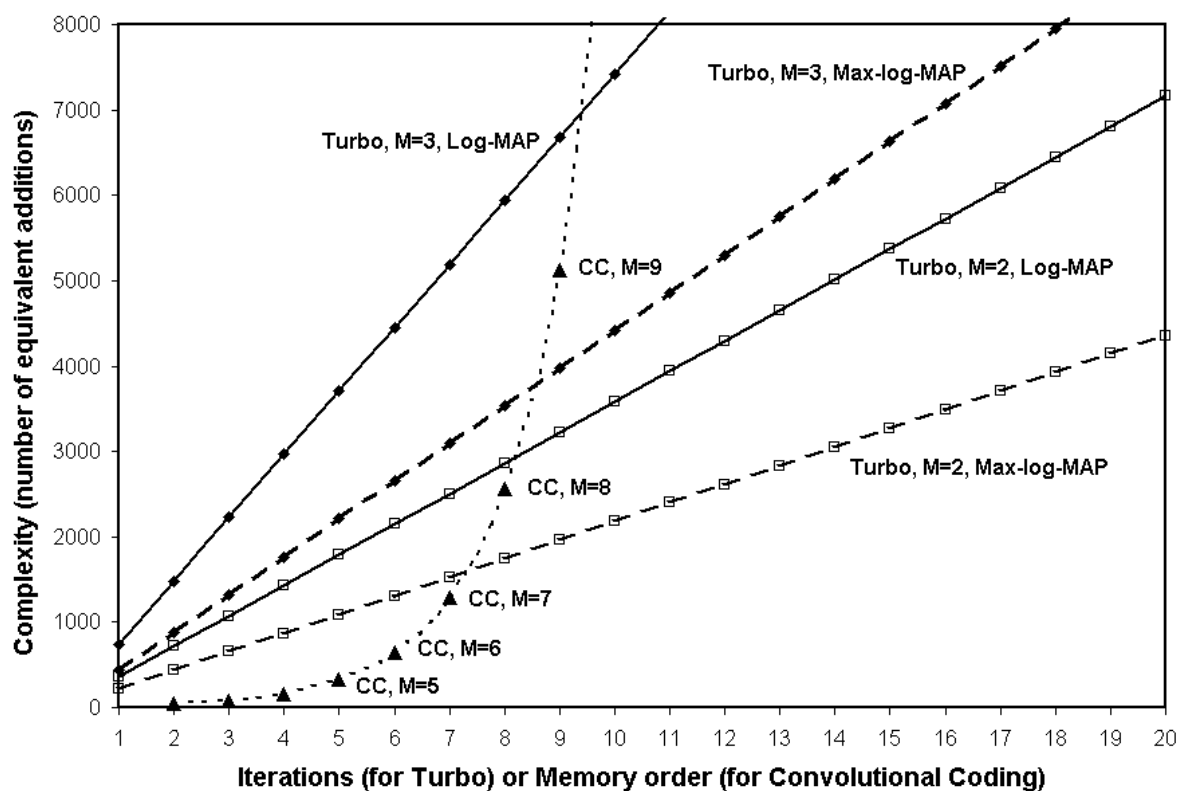


Figure 2: Complexity comparison between turbo decoding and convolutional decoding.

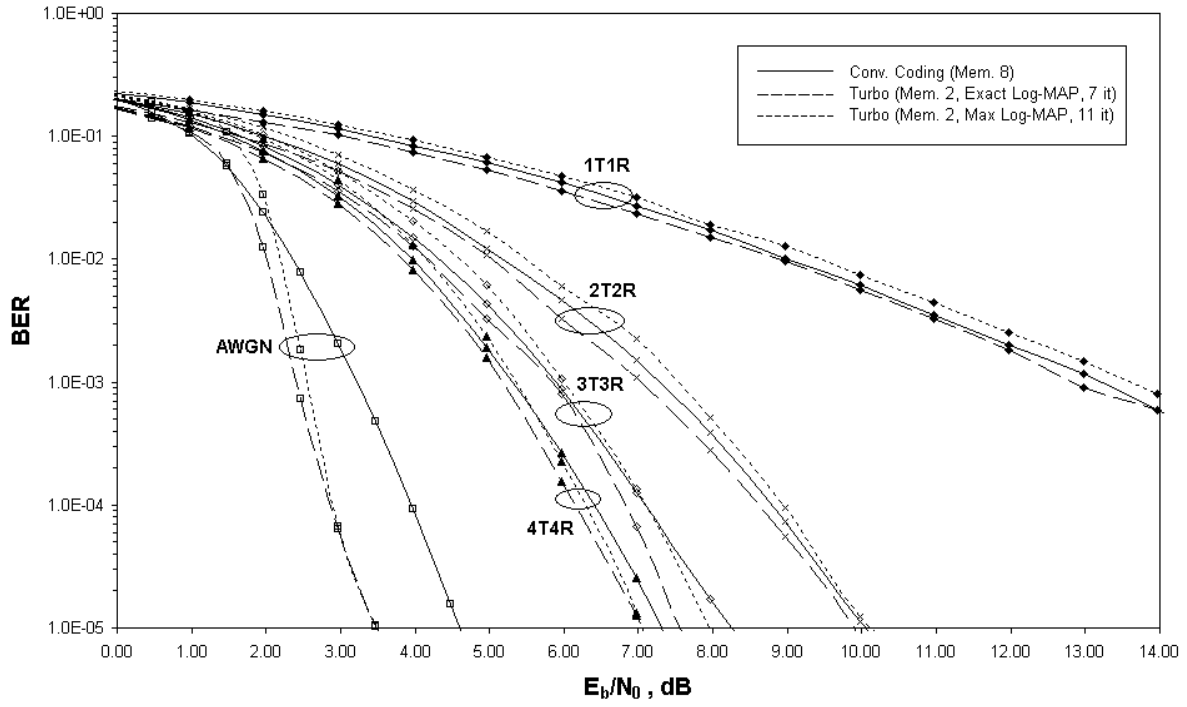


Figure 3: Error rates for various turbo-coded and convolutional-coded OFDM systems for both single and multiple antenna FWA configurations for frames having 2048 code bits. Antenna envelope correlation coefficient is set to 0.4.

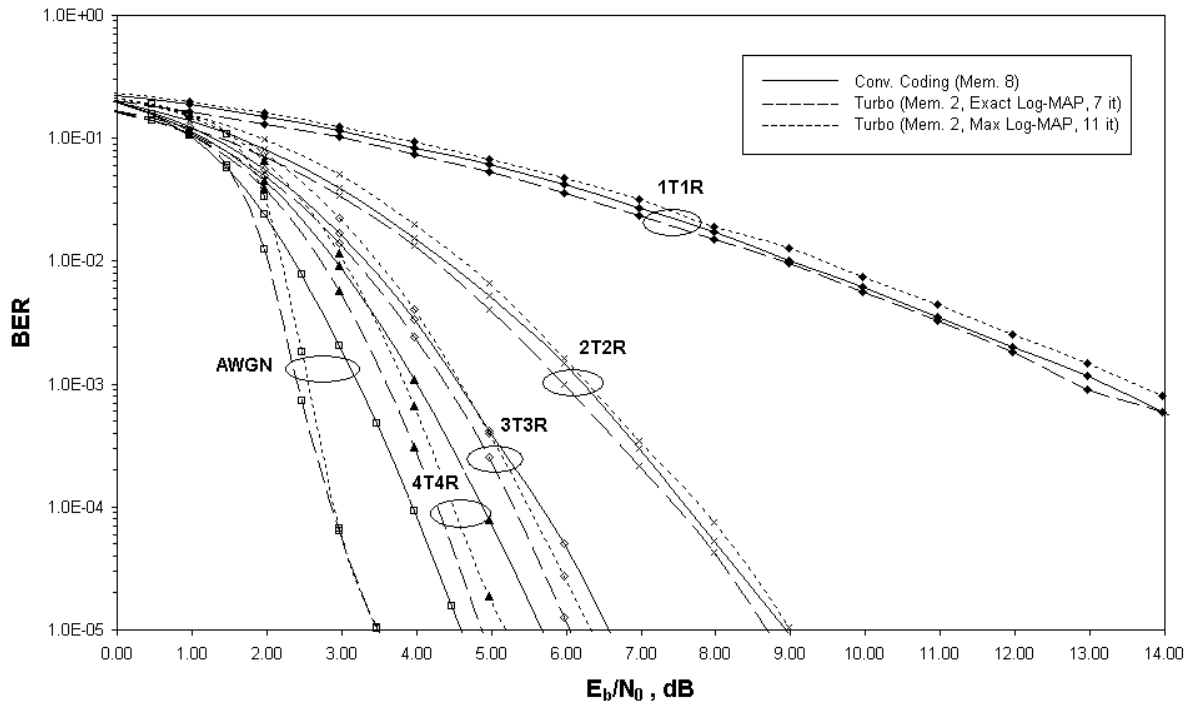


Figure 4: Error rates for various turbo-coded and convolutional-coded OFDM systems for both single and multiple antenna FWA configurations for frames having 2048 code bits. Antenna envelope correlation coefficient set to zero.

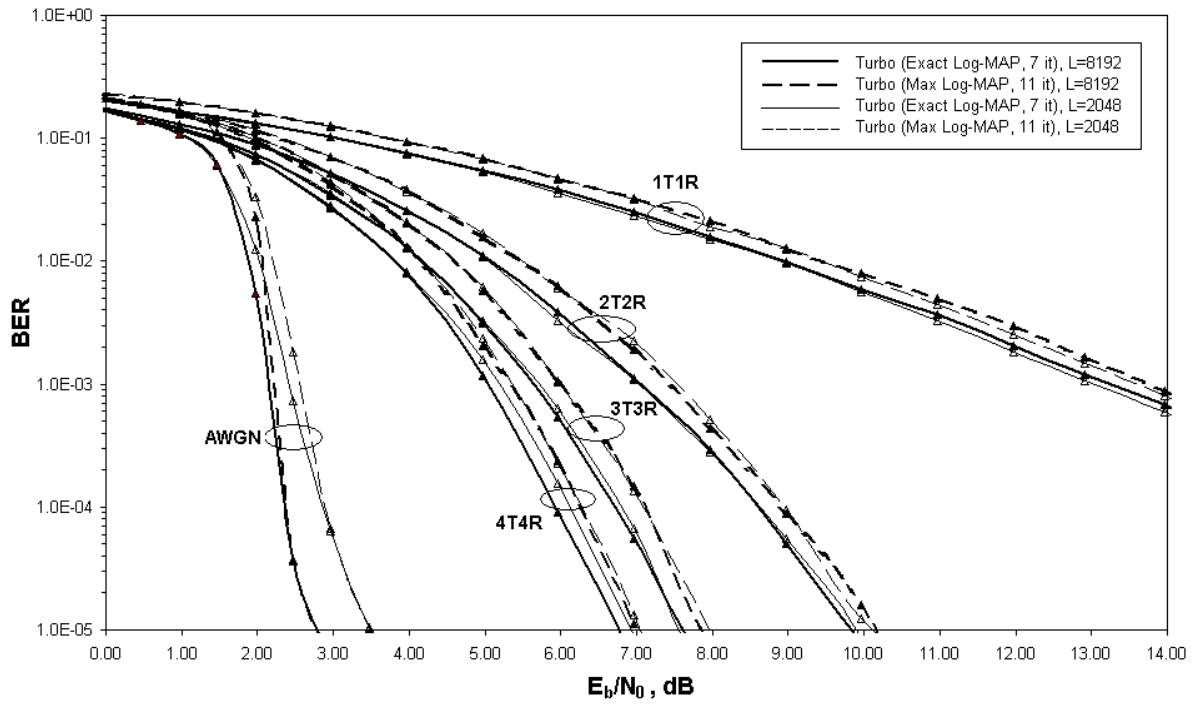


Figure 5: Error rates for turbo-coded OFDM systems for both single and multiple antenna FWA configurations for frames having 2048 or 8192 code bits. Antenna envelope correlation coefficient is set to 0.4.

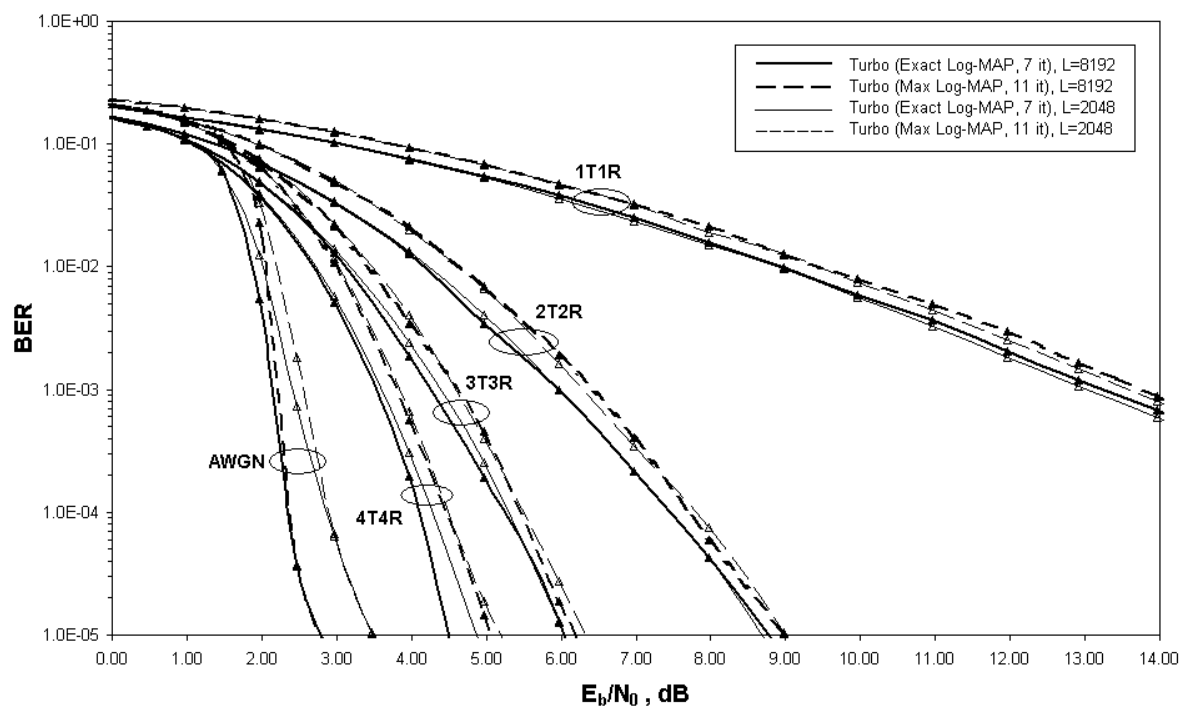


Figure 6: Error rates for turbo-coded OFDM systems for both single and multiple antenna FWA configurations for frames having 2048 or 8192 code bits. Antenna envelope correlation coefficient is set to zero.

Tables

Table 1: Computational requirements of the log-MAP algorithm.

	ADD	SUB	MUL	DIV	MAX	LKUP
Procedure A	4×2^M	–	6×2^M	2×2^M	–	–
Procedure B	3×2^M	2^M	–	–	2^M	2^M
Procedure C	3×2^M	2^M	–	–	2^M	2^M
Procedure D	$6 \times 2^M - 2$	$2 \times 2^M - 1$	–	–	$2 \times (2^M - 1)$	$2 \times (2^M - 1)$

Table 2: Computational requirements of the max-log-MAP algorithm.

	ADD	SUB	MUL	DIV	MAX	LKUP
Procedure A	4×2^M	–	6×2^M	2×2^M	–	–
Procedure B	2×2^M	–	–	–	2^M	–
Procedure C	2×2^M	–	–	–	2^M	–
Procedure D	4×2^M	1	–	–	$2 \times (2^M - 1)$	–

Table 3: Computational requirements of the Viterbi algorithm.

	ADD	SUB	MUL	DIV	MAX	LKUP
Procedure A	2×2^M	–	4×2^M	–	–	–
Procedure E	2×2^M	–	–	–	2^M	–
Procedure G	–	–	–	–	–	1

Table 4: Complexity of the decoding algorithms.

	Number of Equivalent Additions
Log-MAP algorithm	$48 \times 2^M - 13$
Max-log-MAP algorithm	$28 \times 2^M - 3$
Viterbi algorithm	$10 \times 2^M + 3$